Homotopy Perturbation Method for Nonlinear Vibration Analysis of Functionally Graded Plate

Ali A. Yazdi[1]
Department of Mechanical Engineering,
Quchan Institute of Engineering and Technology,
Quchan, P. O. Box 94717-84686, Iran
e-mail: aliaminyazdi@gmail.com

In this paper, the Homotopy perturbation method (HPM) is used to analysis the geometrically nonlinear vibrations of thin rectangular laminated functionally graded material (FGM) plates. The Von Karman's strain-displacement relations have been employed to model structural nonlinearity of the system. The material properties of the plate are assumed to be graded continuously in direction of thickness. The effects of initial deflection, aspect ratio and material properties are investigated. Based on the results of this study, the first order approximation of the HPM leads to highly accurate solutions for geometrically nonlinearity vibration of FGM plates. Moreover, HPM in comparison with other traditional analytical methods (e.g., perturbation methods) has excellent accuracy for the whole range of oscillation amplitude and initial conditions. [DOI: 10.1115/1.4023252]

1 Introduction

The applicability of FGM structural components in design of aerospace structures is extended widely in recent years due to their excellent performance in the high temperature environments. Continuous variation of constituent material's volume fraction is a special property of FGMs that causes the continuous variation of properties. The functionally graded materials are usually made of ceramic and metal to attain the significant requirement of material properties. Due to these outstanding properties, the FGMs have received considerable attention in recent years.

Reddy and Chin [1] developed a finite element model to investigate the dynamic thermo elastic response of FGM cylinders and plates. They used first-order shear deformation plate theory (FSDT) with three dimensional heat conduction to formulate the governing equation of the system.

Cheng and Barta [2] studied the steady state vibration of a simply supported FGM polygonal plate. Ng et al. [3] investigated the dynamic stability of simply supported FGM thin plates under harmonic in-plane loading.

Yang et al. [4] investigated the large amplitude vibration analysis of prestressed FGM laminated plates. The Reddy's higher order shear deformation plate theory was used to obtain the nonlinear governing equations of the system.

Qien et al. [5] conducted an investigation on free and forced vibrations and static deformations of a FGM thick simply supported square plate using a higher order shear and normal deformable plate theory and a mesh-less local Petrov–Galerkin method. Vel and Batra [6] studied analytically the free and forced vibrations of FGM simply supported rectangular plates based on the 3D elasticity solution. Sundararajan et al. [7] developed a nonlinear formulation based on Von Karman's assumptions to study the free vibration characteristic of FGM plates subjected to thermal environment.

Abrate [8] investigated the free vibrations, buckling and static deflections of FGM plates using the classical laminated plate, the FSDT and HSDT models. Hashemi et al. [9] studied free vibration of moderately thick rectangular plates resting on elastic foundations.

In recent years, the Homotopy perturbation method (HPM) as an easy to use analytical tool for solving strongly nonlinear equations has received considerable attention. He [10] presented a new perturbation technique coupled with Homotopy method to solve the strongly nonlinear problems. Sun et al. [11] presented a uniform algorithm to study the eigenvalue problem of a lined duct using the homotopy method.

Blendez et al. [12] used He's Homotopy perturbation method (HPM) to present an approximate solution to conservative truly nonlinear oscillations. Yongqiang et al. [13] used homotopy perturbation method to study the geometrically nonlinear free vibrations of symmetric rectangular honeycomb sandwich panels. Pirbodaghi et al. [14] used HPM to obtain an approximate analytical solution for geometrically nonlinear vibrations of thin laminated composite plates resting on nonlinear elastic foundations.

In this paper the geometrically nonlinear vibration of thin FGM laminated rectangular plate is investigated. The homotopy perturbation method (HPM) is used to obtain approximate analytical solutions. The effect of parameters such as initial deflection, aspect ratio and material properties on frequency ratio is investigated. In all cases in this study, the frequency ratio is defined as the ratio of nonlinear frequency to linear frequency.

2 Problem Description

In Fig. 1, a FGM plate of length a, width b and uniform thickness h, which is made of a ceramic and a metal is considered. It is assumed that material properties are varied through the thickness of the plate according to a simple power law function of the volume fractions of the constituents as follows [1]:

$$P(z) = (P_c - P_m)V_c + P_m \tag{1}$$

$$V_c(z) = \left(\frac{2z+h}{2h}\right)^n (0 \le n \le \infty) \tag{2}$$

where P denotes the effective material properties and subscript m, c refer to metal and ceramic, respectively. Also, V_c is the volume fraction of the ceramic and n is the non-negative exponent of power. According to Eqs. (1) and (2) the effective material properties distribution of the plate through the thickness can be determined as follows [1]:

$$E(z) = (E_c - E_m)\left(\frac{2z+h}{2h}\right)^n + E_m \tag{3}$$

[1]Corresponding author.

Contributed by the Design Engineering Division of ASME for publication in the JOURNAL OF VIBRATION AND ACOUSTICS. Manuscript received July 3, 2012; final manuscript received November 28, 2012; published online March 18, 2013. Assoc. Editor: Mahmoud Hussein.

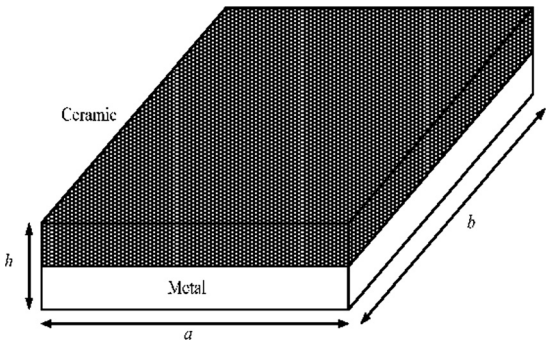

Fig. 1 Geometry of thin rectangular FGM plate

$$v(z) = (v_c - v_m)\left(\frac{2z+h}{2h}\right)^n + v_m \tag{4}$$

$$\rho(z) = (\rho_c - \rho_m)\left(\frac{2z+h}{2h}\right)^n + \rho_m \tag{5}$$

Employing the Von Karman deformation assumption, the strain displacement relations are:

$$\varepsilon_{xx} = \frac{\partial u}{\partial x} + \frac{1}{2}\left(\frac{\partial w}{\partial x}\right)^2 - z\frac{\partial^2 w}{\partial x^2} \tag{6}$$

$$\varepsilon_{yy} = \frac{\partial v}{\partial y} + \frac{1}{2}\left(\frac{\partial w}{\partial y}\right)^2 - z\frac{\partial^2 w}{\partial y^2} \tag{7}$$

$$\varepsilon_{xy} = \frac{1}{2}\left(\frac{\partial u}{\partial y} + \frac{\partial v}{\partial x} + \frac{\partial w}{\partial x}\frac{\partial w}{\partial y}\right) - 2z\frac{\partial^2 w}{\partial x \partial y} \tag{8}$$

$$\varepsilon_{xz} = \varepsilon_{yz} = \varepsilon_{zz} = 0 \tag{9}$$

Based on classical laminated plate theory, the stress-strain relations are

$$\begin{Bmatrix} \sigma_{xx} \\ \sigma_{yy} \\ \sigma_{xy} \end{Bmatrix} = \begin{bmatrix} Q_{11} & Q_{12} & 0 \\ Q_{12} & Q_{22} & 0 \\ 0 & 0 & Q_{66} \end{bmatrix} \begin{Bmatrix} \varepsilon_{xx} \\ \varepsilon_{yy} \\ 2\varepsilon_{xy} \end{Bmatrix} \tag{10}$$

where Q_{ij} stiffness coefficient can be expressed as follows [1]:

$$Q_{11} = Q_{22} = \frac{E(z)}{1 - v(z)^2} \tag{11}$$

$$Q_{12} = \frac{E(z)v(z)}{1 - v(z)^2} \tag{12}$$

$$Q_{66} = \frac{E(z)}{2[1 + v(z)]} \tag{13}$$

According to Eqs. (6)–(13), the force and moment resultants are given by

$$\begin{Bmatrix} N_x \\ N_y \\ N_{xy} \end{Bmatrix} = \int_{-h/2}^{h/2} \begin{Bmatrix} \sigma_{xx} \\ \sigma_{yy} \\ \sigma_{xy} \end{Bmatrix} dz \tag{14}$$

$$\begin{Bmatrix} M_x \\ M_y \\ M_{xy} \end{Bmatrix} = \int_{-h/2}^{h/2} \begin{Bmatrix} \sigma_{xx} \\ \sigma_{yy} \\ \sigma_{xy} \end{Bmatrix} z dz \tag{15}$$

Using Hamilton principle the governing equations of the system obtained [1]:

$$\begin{aligned}
&\frac{\partial N_x}{\partial x} + \frac{\partial N_{xy}}{\partial y} = 0 \\
&\frac{\partial N_y}{\partial y} + \frac{\partial N_{xy}}{\partial x} = 0 \\
&\frac{\partial^2 M_x}{\partial x^2} + 2\frac{\partial^2 M_{xy}}{\partial x \partial y} + \frac{\partial^2 M_y}{\partial y^2} + \frac{\partial}{\partial x}\left(N_x \frac{\partial w}{\partial x}\right) + \frac{\partial}{\partial x}\left(N_{xy}\frac{\partial w}{\partial y}\right) \\
&\quad + \frac{\partial}{\partial y}\left(N_{xy}\frac{\partial w}{\partial x}\right) + \frac{\partial}{\partial y}\left(N_y \frac{\partial w}{\partial y}\right) = I_0 \frac{\partial^2 w}{\partial t^2}
\end{aligned} \tag{16}$$

where

$$I_0 = \int_{-h/2}^{h/2} \rho(z) dz$$

The boundary conditions are as follows:

at $x = 0, a$ $v = w = 0$

at $y = 0, b$ $u = w = 0$

To solve the nonlinear free vibration problem the following set of admissible functions which satisfy the boundary conditions are considered [15]:

$$\begin{aligned}
u &= U(t)\cos\frac{m\pi}{a}x \sin\frac{n\pi}{b}y \\
v &= V(t)\sin\frac{m\pi}{a}x \cos\frac{n\pi}{b}y \\
w &= W(t)\sin\frac{m\pi}{a}x \sin\frac{n\pi}{b}y
\end{aligned} \tag{17}$$

where $U(t)$, $V(t)$ and $W(t)$ are the maximum displacements in x, y and z directions, respectively. Applying Galerkin method to Eqs. (16) and substituting $U(t)$ and $V(t)$ in terms of $W(t)$ obtained from the first two equations, into the third equation results in the single second-order ordinary differential equation in $W(t)$:

$$\frac{d^2W(t)}{dt^2} + \alpha W(t) + \beta W(t)^2 + \gamma W(t)^3 = 0 \tag{18}$$

where α, β and γ are coefficients that depend on the plate stiffness and dimensions and are defined in the Appendix A. The center of the plate is subjected to the following initial conditions:

$$W(0) = W_{\max}, \quad \frac{dW(0)}{dt} = 0 \tag{19}$$

where $W_{\max}$ is the maximum vibration amplitude of the plate center. In order to solve the nonlinear differential equation (Eq. (18)) the homotopy perturbation method is used. By the homotopy technique a homotopy $w(r,p) : \Omega \times [0,1]$, which satisfies the following expression is constructed [10]:

$$H(w,p) = L(w) - L(u_0) + pL(u_0) + pN(w) = 0 \tag{20}$$

where L and N are linear and nonlinear parts of Eq. (18) and u_0 is initial approximation of Eq. (18), which satisfies the initial conditions. Assuming the solution of Eq. (18) as a power series we have [10]:

$$w = w_0 + pw_1 + p^2 w_2 + \ldots \tag{21}$$

The substitution of Eqs. (21) into (20) yields:

$$\begin{aligned}
L(w_0) - L(u_0) &= 0 \\
w_0 = W_{\max}, \quad \frac{dw_0}{dt} &= 0
\end{aligned} \tag{22}$$

$$\begin{aligned}
L(w_1) - L(u_1) + \beta w_0^2 + \gamma w_0^3 &= 0 \\
w_1(0) = \frac{dw_1(0)}{dt} &= 0
\end{aligned} \tag{23}$$

In order to satisfy the initial conditions, the initial guess of u_0 is chosen as follows:

$$w_0(t) = u_0(t) = W_{\max}\cos(\omega t) \tag{24}$$

Therefore from Eq. (23) we have:

$$\frac{d^2w_1}{dt^2} + \alpha w_1 + W_{\max}\left(\alpha - \omega^2 + \frac{3}{4}W_{\max}^2\gamma\right)\cos(\omega t) + \frac{\beta W_{\max}^2}{2}\cos(2\omega t) + \frac{\gamma W_{\max}^3}{4}\cos(3\omega t) + \frac{\beta W_{\max}^2}{2} = 0 \tag{25}$$

The solution of Eq. (25) can be obtained by variational iteration method:

$$w_1(t) = \frac{1}{\alpha}\int_0^t \sin(\tau - t)\left[W_{\max}\left(\alpha - \omega^2 + \frac{3}{4}W_{\max}^2\gamma\right)\cos(\omega\tau) + \frac{\beta W_{\max}^2}{2}\cos(2\omega\tau) + \frac{\gamma W_{\max}^3}{4}\cos(3\omega\tau) + \frac{\beta W_{\max}^2}{2}\right]d\tau \tag{26}$$

$$w_1(t) = W_{\max}\left(\alpha - \omega^2 + \frac{3}{4}W_{\max}^2\gamma\right)\left(\frac{\alpha}{\omega^2 - \alpha^2}\right)\cos(\omega t) + \frac{\beta W_{\max}^2}{2}\left(\frac{\alpha}{4\omega^2 - \alpha^2}\right)\cos(2\omega t) + \frac{\gamma W_{\max}^3}{4}\left(\frac{\alpha}{9\omega^2 - \alpha^2}\right) \times \cos(3\omega t) - \frac{\beta W_{\max}^2}{2\alpha} + \left[W_{\max}\left(\alpha - \omega^2 + \frac{3}{4}W_{\max}^2\gamma\right) \times \frac{\alpha}{\alpha^2 - \omega^2} + \left(\frac{\beta W_{\max}^2}{2}\right)\frac{\alpha}{\alpha^2 - 4\omega^2} + \left(\frac{\gamma W_{\max}^3}{4}\right)\frac{\alpha}{\alpha^2 - 9\omega^2} + \left(\frac{\beta W_{\max}^2}{2\alpha}\right)\right]\cos\alpha t \tag{27}$$

In order to identify ω the secular term should be eliminated. Set the coefficient of $\cos(\alpha t)$ to zero yields the following equation:

$$g_1\omega^6 + g_2\omega^4 + g_3\omega^2 + g_4 = 0 \tag{28}$$

The coefficients g_i are listed in Appendix B. Manipulating Eq. (28) gives one cubic equation in ω^2 with stiffness and dimensions of FGM plate as parameters. Thus, the first-order approximation of the $W(t)$ become as follows:

$$W(t) \approx w_0(t) + w_1(t) = W_{\max}\left(\frac{\omega^2(1-\alpha) + 3/4W_{\max}\gamma\alpha}{\omega^2 - \alpha^2}\right)\cos(\omega t) + \frac{\beta W_{\max}^2}{2}\left(\frac{\alpha}{4\omega^2 - \alpha^2}\right)\cos(2\omega t) + \frac{\gamma W_{\max}^3}{4}\left(\frac{\alpha}{9\omega^2 - \alpha^2}\right) \times \cos(3\omega t) - \frac{\beta W_{\max}^2}{2\alpha}$$

In Sec. 3, the accuracy of the presented method is discussed in detail.

3 Results and Discussion

The analysis is performed for pure materials and different values of volume fraction exponent, n, for aluminum-zirconia FGM. The properties of FGM components are presented in Table 1. To validate the present formulation and ensure the accuracy and convergence of the proposed solution method, the nonlinear vibrations of thin laminated composite plates are first solved. Direct comparisons have been carried out with results that are available in the previous works [15].

According to Table 2, a good agreement was shown between the present results and the results obtained by Singh et al. [15]. These data validate the capability of the present method for reliable prediction of nonlinear frequency of thin rectangular FGM plate.

Table 1 Properties of FGM components

	Properties		
Materials	E(N/m^2)	v	$\rho(Kg/m^3)$
Aluminum (Al)	70×10^9	0.3	2700
Zirconia (ZrO_2)	151×10^9	0.3	3000

Table 2 Comparison of nonlinear to linear frequency ratio for thin cross-ply laminated plates

	$(0/90)_s$, a/b = 1		$(0/90)_2$, a/b = 2	
$W_{\max}/h$	Singh et al. [15]	Present study	Singh et al. [15]	Present study
0.25	1.0535	1.0547	1.0645	1.0679
0.5	1.2038	1.2167	1.2427	1.2563
0.75	1.4172	1.432	1.4905	1.4221
1	1.6691	1.7119	1.7787	1.7818
1.5	2.2355	2.2825	2.4178	2.4768
2	2.8439	2.9129	3.0976	3.1332

Table 3 Nonlinear to linear frequency ratio for square laminated FGM plate (*a/h* = 40)

	n					
$W_{\max}/h$	0.2	0.5	2	5	10	100
0.25	1.0467	1.0470	1.0437	1.0413	1.0413	1.0447
0.5	1.1758	1.1768	1.1652	1.1563	1.1563	1.1686
0.75	1.3641	1.3661	1.3436	1.3262	1.3266	1.3502
1	1.5911	1.5941	1.5596	1.5329	1.5335	1.5697
1.25	1.8426	1.8467	1.8	1.7637	1.7645	1.8137
1.5	2.1103	2.1154	2.0564	2.0106	2.0115	2.0738
1.75	2.3890	2.3952	2.3239	2.2684	2.2996	2.3449
2	2.6755	2.6828	2.5993	2.5342	2.5355	2.6239

Table 4 Nonlinear to linear frequency ratio for rectangular laminated FGM plate (*a/b* = 2)

	n					
$W_{\max}/h$	0.2	0.5	2	5	10	100
0.25	1.0457	1.0461	1.0432	1.0406	1.0405	1.0436
0.5	1.1721	1.1736	1.1632	1.1539	1.1535	1.1649
0.75	1.3572	1.3602	1.3397	1.3214	1.3208	1.3431
1	1.5809	1.5854	1.5539	1.5258	1.5248	1.5593
1.25	1.8294	1.8356	1.7928	1.7545	1.7531	1.8001
1.5	2.0946	2.1024	2.0483	1.9996	1.9979	2.0574
1.75	2.3715	2.381	2.3153	2.2562	2.2541	2.3264
2	2.6571	2.6684	2.591	2.5213	2.5188	2.604

Tables 3–5 show the obtained results of frequency ratio for a laminated FGM plate having three different aspect ratios. As it can be seen, by increasing the vibration amplitude the difference between nonlinear and linear frequency is increased. In other word, the discrepancy between nonlinear and linear frequency is deeply depend on the vibration amplitude. Additionally, it should be noted that in all cases for $n = 0.5$, a higher frequency ratio is obtained. Additionally, it should be noted that the plates with larger aspect ratios can affect the frequency ratio significantly. This can be attributed to this fact that the effect of aspect ratio on nonlinear terms (β, γ) in Eq. (18) is more considerable.

Table 5 Nonlinear to linear frequency ratio for rectangular laminated FGM plates ($a/b = 4$)

	n					
W_{max}/h	0.2	0.5	2	5	10	100
0.25	1.0497	1.0503	1.0444	1.0444	1.0442	1.0475
0.5	1.1865	1.1884	1.1777	1.1673	1.1667	1.1787
0.75	1.3848	1.3885	1.3677	1.3476	1.3464	1.3697
1	1.6223	1.6278	1.5962	1.5656	1.5637	1.5992
1.25	1.8841	1.8916	1.8491	1.8076	1.8050	1.8531
1.5	2.1616	2.171	2.1175	2.0654	2.0621	2.1226
1.75	2.4494	2.4608	2.3965	2.3336	2.3297	2.4026
2	2.7444	2.7577	2.6826	2.6092	2.6046	2.6897

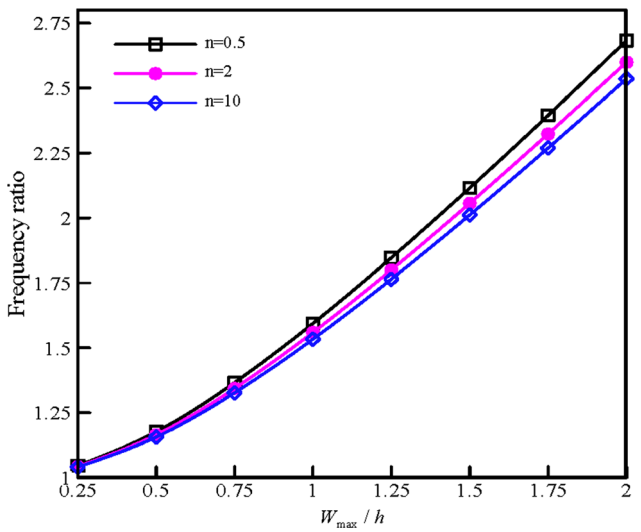

Fig. 2 Variation of frequency ratios versus nondimensional amplitude ratio for square FGM plate for different n

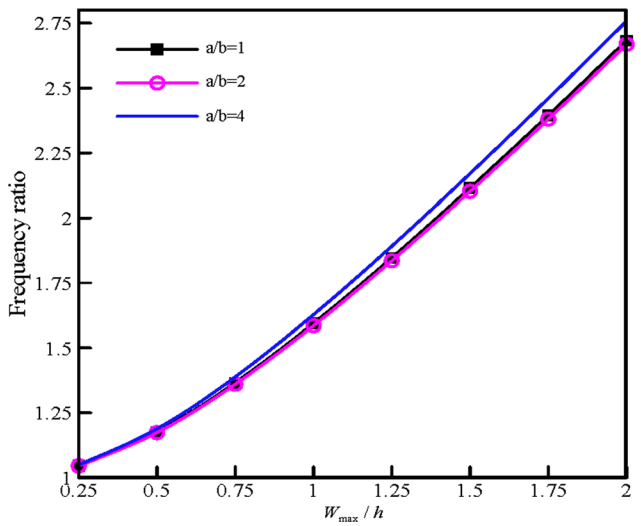

Fig. 3 Variation of frequency ratios versus nondimensional amplitude ratio for square FGM plate with different aspect ratios

In Figs. 2 and 3, the variation of frequency ratios versus vibration amplitude for different values of n and aspect ratios are presented, respectively. As it is shown all response curves exhibit initial softening trends and revert to hardening amplitudes at large amplitudes although the degree of hardening vary. As it was

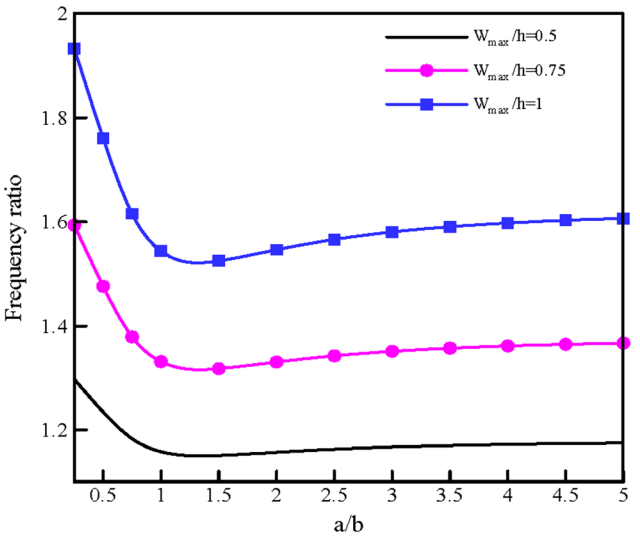

Fig. 4 Effect of aspect ratio on frequency ratio for different vibration amplitude

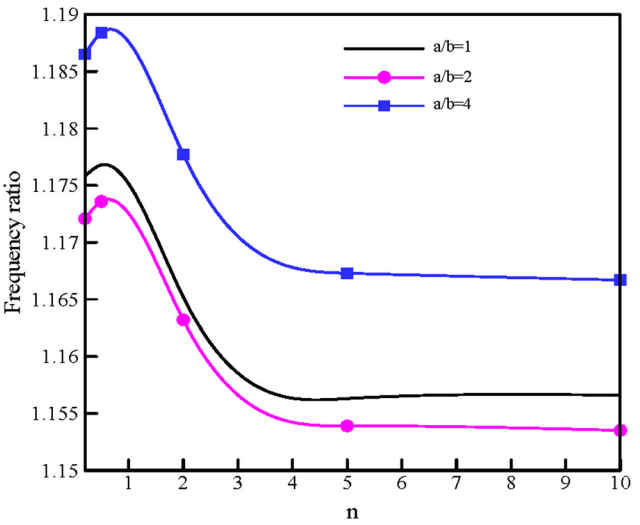

Fig. 5 Variation of frequency ratio versus the different values of n for $W_{max}/h = 0.5$

shown in Fig. 2, by increasing the vibration amplitude the frequency ratio is increased consequently. On the other hand, increasing the value of n results the reduction of frequency ratio. In similar way, in Fig. 3 for plates with different aspect ratios, similar result can be concluded. It can be concluded from Fig. 3 that increasing the aspect ratio yields a higher frequency ratio for rectangular FGM plate ($a/b = 4$) in comparison with square one.

Figure 4 demonstrates the effect of aspect ratio on frequency ratio for three different vibration amplitudes. As it can be seen, for $0.25 < a/b < 1.5$, increasing the aspect ratio results the reduction of frequency ratio while for bigger values of aspect ratios, the results convergent to specific value. This property can also be reflected in Fig. 3.

Figure 5 shows the effect of different values of n on frequency ratio. As it can be seen, with increasing the values of n, for $0.25 < n < 1$, the frequency ratio is decreased while for $n > 1$, it approximately remains constant. This behavior can be attributed to this fact, that increasing the values of n results the reduction ρ, A_{ij} and D_{ij} (i, $j = 1$, 2, 6), while the coupling stiffness B_{ij} is increased. Additionally, it should be noted that the discrepancy of the above properties with enhancement of n, is more considerable for $n < 1$, while for $n > 1$ this variation is very negligible.

Table 6 Effect of material properties on frequency ratio of laminated FGM square plate

	Materials			
W_{max}/h	Alumina (Al_2O_3)	Zirconia (ZrO_2)	Ti-6Al-4 V	Stainless steel (SUS304)
0.25	1.0483	1.047	1.0466	1.0478
0.5	1.1815	1.1768	1.1754	1.1796
1	1.6084	1.5941	1.5924	1.6047
1.5	2.1405	2.1154	2.1197	2.1409
1.75	2.4261	2.3952	2.4066	2.4322
2	2.7199	2.6828	2.7054	2.7356

Table 6 illustrates the effect of material properties on frequency ratio of FGM plate. As it can be seen the E_U/E_L ratio plays significant role in predicting frequency ratio. As it can be seen with increasing the E_U/E_L ratio, the frequency ratio is increased consequently.

4 Conclusions

In this study, the homotopy perturbation method (HPM) is employed to present an approximate-analytical method solution for free nonlinear vibration of thin rectangular laminated FGM plates. Based on iteration method, an expression is introduced for the natural frequency of the FGM plate. The presented expression, unlike other solutions achieved by other techniques, is capable to predict results for large amplitude vibrations. Comparing the results with those obtained by other published works, has been shown the excellent accuracy of first-order approximation of homotopy perturbation method in predicting frequency ratio. In other words, this paper indicates that HPM can be used as a convenient mathematical tool for solving nonlinear differential equation with quadratic and cubic nonlinearities with high accuracy.

Appendix A

$$\alpha = \frac{\left(T_8 + \frac{2T_1T_2T_5 - T_3T_5^2 - T_6T_1^2}{T_3T_6 - T_2^2}\right)}{\left(\sum_{i=1}^{N} \rho_i h_i\right)} \tag{A1}$$

$$\beta = \frac{\left(T_9 + 3\frac{T_2T_4T_5 + T_1T_2T_7 - T_3T_5T_7 - T_1T_4T_6}{T_3T_6 - T_2^2}\right)}{\left(\sum_{i=1}^{N} \rho_i h_i\right)} \tag{A2}$$

$$\gamma = \frac{\left(T_{10} + 2\frac{2T_2T_4T_7 - T_3T_7^2 - T_6T_4^2}{T_3T_6 - T_2^2}\right)}{\left(\sum_{i=1}^{N} \rho_i h_i\right)} \tag{A3}$$

where

$$T_1 = -\left(\frac{n\pi}{b}\right)^3 B_{22} \tag{A4}$$

$$T_2 = \left(\frac{m\pi}{a}\right)\left(\frac{n\pi}{b}\right)(A_{12} + A_{66}) \tag{A5}$$

$$T_3 = \left(\frac{m\pi}{a}\right)^2 A_{66} + \left(\frac{n\pi}{b}\right)^2 A_{22} \tag{A6}$$

$$T_4 = -\frac{4}{9mn\pi^2}\left[\left(\frac{n\pi}{b}\right)^3 A_{22} + \left(\frac{m\pi}{a}\right)^2\left(\frac{n\pi}{b}\right)(A_{12} - A_{66})\right] \tag{A7}$$

$$T_5 = -\left(\frac{m\pi}{a}\right)^3 B_{11} \tag{A8}$$

$$T_6 = \left(\frac{m\pi}{a}\right)^2 A_{11} + \left(\frac{n\pi}{b}\right)^2 A_{66} \tag{A9}$$

$$T_7 = -\frac{4}{9mn\pi^2}\left[\left(\frac{n\pi}{b}\right)^3 A_{11} + \left(\frac{m\pi}{a}\right)\left(\frac{n\pi}{b}\right)^2(A_{12} - A_{66})\right] \tag{A10}$$

$$T_8 = \left(\frac{m\pi}{a}\right)^4 D_{11} + 2\left[\left(\frac{m\pi}{a}\right)^2\left(\frac{n\pi}{b}\right)^2(D_{12} + 2D_{66})\right] + \left(\frac{n\pi}{b}\right)^4 D_{22} \tag{A11}$$

$$T_9 = -\frac{4c_{mn}}{9mn\pi^2}\left[\left(\frac{m\pi}{a}\right)^4 B_{11} + \left(\frac{n\pi}{b}\right)^4 B_{22}\right] \tag{A12}$$

$$T_{10} = \frac{9}{32}\left[\left(\frac{m\pi}{a}\right)^4 A_{11} + \left(\frac{n\pi}{b}\right)^4 A_{22}\right] + \frac{1}{16}\left(\frac{m\pi}{a}\right)^2\left(\frac{n\pi}{b}\right)^2(A_{12} + 2A_{66}) \tag{A13}$$

where

$$(A_{ij}, B_{ij}, D_{ij}) = \int_{-h/2}^{h/2} Q_{ij}(1, z, z^2)dz \; i = j = 1, 2, 6 \tag{A14}$$

$$I_0 = \int_{-h/2}^{h/2} \rho(z)dz \tag{A15}$$

Appendix B

$$g_1 = 36W_{max}\left(\frac{\beta W_{max}}{2\alpha^2} - 1\right) \tag{B1}$$

$$g_2 = W_{max}\left[\alpha^2\left(13 - \frac{49\beta W_{max}}{2}\right) - 36\alpha + \frac{9\beta W_{max}}{2} - 26\gamma W_{max}\right] \tag{B2}$$

$$g_3 = -W_{max}\left[\alpha^4 + 13\alpha^3 - \left(2\beta W_{max} - 11\gamma W_{max}^2\right)\alpha^2\right] \tag{B3}$$

$$g_4 = \alpha^4 W_{max}\left(\alpha + \gamma W_{max}^2\right) \tag{B4}$$

References

[1] Reddy, J. N., and Chin, C. D., 1998, "Thermo Mechanical Analysis of Functionally Graded Cylinders and Plates," J. Therm. Stress., **21**(6), pp. 593–626.
[2] Cheng, Z. Q., and Barta, R. C., 2000, "Exact Correspondence Between Eigenvalues of Membranes and Functionally Graded Simply Supported Polygonal Plates," J. Sound Vib., **229**, pp. 879–895.
[3] Ng, T. Y., Lam, K. Y., and Liew, K. M., 2000, "Effects of FG Materials on the Parametric Resonance of Plate Structures," Comput. Methods Appl. Mech. Eng., **190**, pp. 953–962.
[4] Yang, J., Kitipornchai, S., and Liew, K. M., 2003, "Large Amplitude Vibration of Thermo-Electro-Mechanically Stressed FGM Laminated Plates," Comput. Methods Appl. Mech. Eng., **192**, pp. 3861–3885.
[5] Qien, L. F., Batra, R. C., and Chen L. M., 2004, "Static and Dynamic Deformations of Thick Functionally Graded Elastic Plate by Using Higher-Order Shear and Normal Deformable Plate Theory and Mesh Less Local Petrov-Galerkin Method," Comps. Part B Eng., **35**, pp. 685–697.
[6] Vel, S. S., and Batra, R. C., 2004, "Three-Dimensional Exact Solution for the Vibration of Functionally Graded Rectangular Plates," J. Sound Vib., **272**, pp. 703–730.
[7] Sundararajan, N., Prakash, T., and Ganapathi, M., 2005, "Nonlinear Free Flexural Vibrations of Functionally Graded Rectangular and Skew Plates Under Thermal Environments," Finite Elements Anal. Des., **42**, pp. 152–168.
[8] Abrate, S., 2006, "Free Vibration Buckling and Static Deflections of Functionally Graded Plates," Comput. Sci. Technol., **66**, pp. 2383–2394.
[9] Hashemi, Sh. H., Taher, H. R. D., Akhavan, H., and Omidi, M., 2010, "Free Vibration of Functionally Graded Rectangular Plates Using First-Order Shear Deformation Plate Theory," Appl. Math. Model., **34**, pp. 1276–1291.
[10] He, J. H., 1999, "Homotopy Perturbation Technique," Comput. Meth. Appl. Mech. Eng., **178**, pp 257-262.
[11] Sun, X., Du, L., and Yang, V., 2007, "A Homotopy Method for Determining the Eigenvalues of Locally or Non-Locally Reacting Acoustic Liners in Flow Ducts," J. Sound Vib., **303**, pp. 277–286.

[12] Blendez, A., Blendez, T., Marquez, A., and Niepp, A., 2008, "Application of He's Homotopy Perturbation Method to Conservative Truly Non-Linear Oscillators," Chaos, Solitons Fractals, **37**(3), pp. 770–780.
[13] Yongqiang, L., Feng, L., and Dawei, Z., 2010, "Geometrically Non-Linear Free Vibrations of the Symmetric Rectangular Honeycomb Sandwich Panels With Simply Supported Boundaries," Compos. Struct., **92**, pp. 1110–1119.
[14] Pirbodaghi, T., Fesanghary, M., and Ahmadian, M.T., 2011, "Non-Linear Vibration Analysis of Laminated Composite Plates Resting on Non-Linear Elastic Foundations," J. Franklin Inst., **348**, pp. 353–368.
[15] Singh, G., Raju, K.K., Rao, G.V., 1990, "Non-Linear Vibrations of Simply Supported Rectangular Cross-Ply Plates," J. Sound Vib., **142**, pp. 213–226.